OPEN ACCESS

University of BRISTOL

Stokes, J. L., Sarua, A., Pugh, J. R., Dorh, N., Munns, J. W., Bassindale, P. G., Ahmad, N., Orr-Ewing, A. J., & Cryan, M. J. (2015). Purcell enhancement and focusing effects in plasmonic nanoantenna arrays. *Journal of the Optical Society of America B*, *32*(10), 2158-2163. https://doi.org/10.1364/JOSAB.32.002158

Peer reviewed version

Link to published version (if available):
10.1364/JOSAB.32.002158

Link to publication record in Explore Bristol Research
PDF-document

© 2015 Optical Society of America

University of Bristol - Explore Bristol Research
General rights

This document is made available in accordance with publisher policies. Please cite only the published version using the reference above. Full terms of use are available:
http://www.bristol.ac.uk/red/research-policy/pure/user-guides/ebr-terms/

Purcell Enhancement and Focusing Effects in Plasmonic Nanoantenna Arrays

J. L. Stokes[1], A. Sarua[2], J. R. Pugh[1], N. Dorh[1], J. W. Munns[2], P. G. Bassingdale[3], N. Ahmad[1], A.J.Orr-Ewing[4] and M. J. Cryan[1].

[1]*Photonics Research Group, Department of Electrical and Electronic Engineering,*
[2]*School of Physics,* [3]*Department of Mechanical Engineering,* [4]*School of Chemistry*
University of Bristol, Bristol, BS8 1UB, UK.
E-Mail: j.stokes@bristol.ac.uk, m.cryan@bristol.ac.uk

Abstract: This paper presents measured fluorescence results for PMMA-dye coated 5 x 5 gold plasmonic nanoantenna arrays. The paper uses numerical electromagnetic modelling to show how array size and element spacing can be used to control emitted beamshape and compares this with experimental data. The Friis formula from RF antenna theory is used to calculate the intensity enhancement produced by the array. A figure-of-merit is then developed which accounts for the very small mode volume from which the array emission is occurring.

1. Introduction

Plasmonic nanoantennas are of considerable interest for use in single molecule detection and sensing applications where they resonantly enhance fluorescent emission from dye molecules, and very large enhancements have been measured in the literature [1], [2]. This is known as Purcell enhancement, first identified by E. Purcell who showed the that electromagnetic environment which surrounds an emitter strongly affects the emission of radiation [3]. Furthermore, nanoantennas can be used to beamshape or focus the radiation from the molecules which can increase the field intensity in the measurement plane and therefore improve detection single-to-noise ratio [4]. Nanoantennas are typically made from conductive material such as noble metals which can have significant optical losses which limits Purcell enhancement. It may be possible to use focusing effects to overcome these loss limitations and this paper studies both Purcell enhancement and focusing effects in an array of gold nanoantennas [5]. Previous work has shown that in order to achieve high field enhancements extremely small gaps are required which are very difficult and therefore expensive to reliably fabricate [6]. This work shows that by utilising array effects larger gaps can be used whilst maintaining large enhancement factors. This paper measures fluorescent emission from a PMMA-dye coated 5 x 5 array of two–arm dipole antennas and shows beam shaping effects which are related to antenna element spacing. A scanning confocal microscope is used to measure the emission and we use 3D Finite Difference Time Domain (FDTD) simulations of 3 x 3 and 5 x 5 arrays to interpret the measured results in terms of array beamshaping effects. The paper then uses the Friis formula from RF antenna theory [7] combined with array gain estimated from FDTD modelling to calculate the power enhancement produced by the array. The Friis formula calculates the power transfer between two antennas of known gain separated by a distance, d at a wavelength,λ. In our case we have two sets of measurements one with and one without the array, since d, λ and the receiving optics are fixed, with an estimate of array gain we can calculate the increase in power produced by the array. This in effect separates Purcell enhancement which occurs at each individual antenna from the collective focusing effect of the array. The paper then introduces a figure-of-merit in order to allow fair comparison between the array and non-array measurements based on an estimate of the array mode volume.

A number of recent publications have investigated radiation pattern manipulation but each only investigates the beamshape from a single element such as a nanocube or single antenna [8], [9]. This paper on the other hand, modifies the emission pattern of fluorescent molecules

using a 2D array of antennas and progresses further to separate Purcell effect from array beamshaping enhancement. Here we use dipole nanoantennas, which consist of two coupled arms that are separated by a small distance, typically 10's of nanometers. This creates high field intensities in the gap region which results in an extremely small mode volume, well below the diffraction limit. This makes the dipole antenna an excellent choice for coupling to fluorescent molecules, as small mode volume is an essential requirement for Purcell enhancement. Furthermore, this type of antenna has been widely used in the RF domain to provide controllable beamshaping. Thus dipole antennas are ideal for combining Purcell and beamshaping effects, though it should be noted that in terms of fabrication, maintaining uniform gaps throughout the 25 elements of a 5 x 5 array remains a significant challenge.

Section 2 describes the fabrication procedure using Focused Ion Beam etching and measurements using scanning confocal microscope. Section 3 shows FDTD modelling of 3 x 3 and 5 x 5 arrays. Section 4 uses FDTD to analyse array gain using the Friis formula which enables an estimate intensity enhancement to be made. Our figure-of-merit based on mode volume is then introduced and calculations are performed to compare the array and non-array results and Section 5 draws conclusions.

2. Fabrication and Measurement

All nanoantennas in this paper are fabricated on gold coated glass substrates from Platypus Technologies [10]. The fabrication of the nanostructures is performed using the Focused Ion Beam (FIB) etching technique [11]. To achieve repeatable nanoantennas it was necessary to create a five step procedure. (i) A C-shape etch is performed with a relatively high ion beam current of 50 pA to create an isolated arm into which the array will be etched, (ii) An etch is performed at 4 pA to leave thin fingers of Au shown in Figure 1(a), (iii) The fingers are then polished to leave uniform edges and to remove re-deposition of Au around the antennas, shown in Figure 1(b), (iv) A vertical etch is performed to create the *x*-axis pitch and gaps between the antenna arms, shown in Figure 1(c). (v) The final etch removes the remaining arm of Au, leaving antennas isolated from the remaining Au on the sample as shown in Figure 1(d).

The nominal dimensions of the fabricated antennas arms are 100 x 40 x 50nm (length x width x thickness) with a gap of 50 nm with a horizontal (*x*) and vertical (*y*) centre-to-centre element spacing of 450 nm and 230 nm respectively.

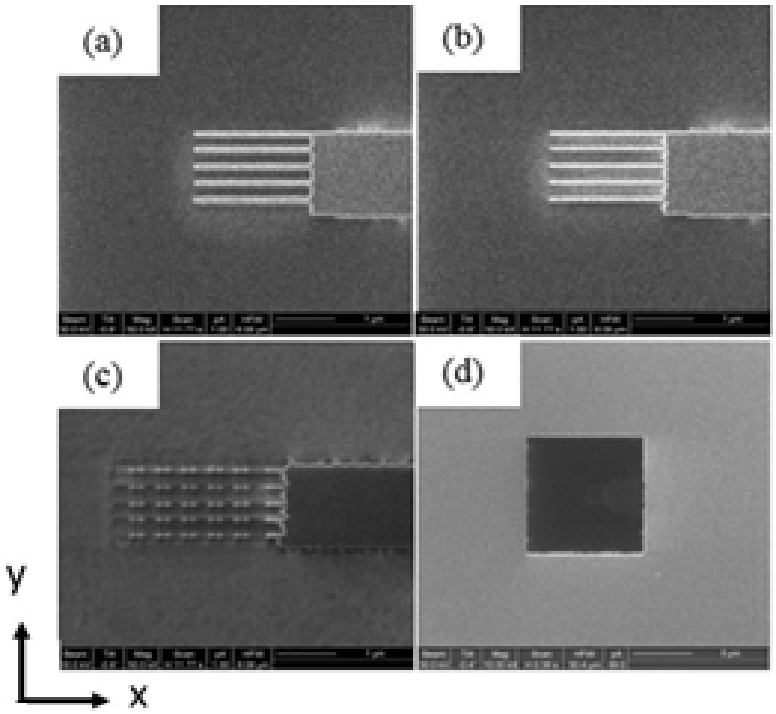

Figure 1 – Images of the array fabrication process (a) Fingers after second etch. (b) Fingers after polishing. (c) Antennas next to remaining Au arm with horizontal (x) and vertical (y) centre-to-centre element spacing of 450 nm and 230 nm respectively. (d) Arm removed and image of whole area.

In order to introduce a fluorescent dye into the antenna array it is most straightforward to mix a dye with a polymer such as PMMA and then use a spin coating process to obtain a thin, flat layer of polymer which evenly coats the whole sample [12]. The dye molecule used is LDS 798 from Photonic Solutions [13]. When the dye is mixed with PMMA the emission band is blueshifted and this shift has been considered when designing the nanoantenna array in order to ensure that an overlap exists with the resonance of the antennas. Figure 2 shows the measured emission spectrum from the dye mixed with PMMA, the FDTD simulated resonance of a dipole antenna with two arms of length 100 nm, width of 40 nm and thickness of 50 nm with a gap of 50 nm and a 5 x 5 array of the same antennas with horizontal (*x*) and vertical (*y*) centre-to-centre element spacing of 450 nm and 230 nm respectively. In the FDTD model the antennas are excited using a plane wave from the air. The dye/PMMA layer is accounted for by covering the antennas with a layer of dielectric with a thickness of 250 nm and a refractive index of n = 1.485 [14]. As expected this layer redshifts the antenna resonance significantly, a redshift of 152 nm is found for a single antenna and 89 nm for a 5 x 5 array. When moving from a single antenna to an array, mutual coupling effects between the elements can be seen to shift the resonant frequency. This is dependent on element spacing and shows that knowledge of the single element response is not sufficient for array design. Figure 2 shows that there is significant overlap between the dye emission peak and the 5 x 5 nanoantenna array resonance peak which should enable emission enhancement to occur. It should be noted that this overlap is not ideal, so that further improvement in future results can be expected.

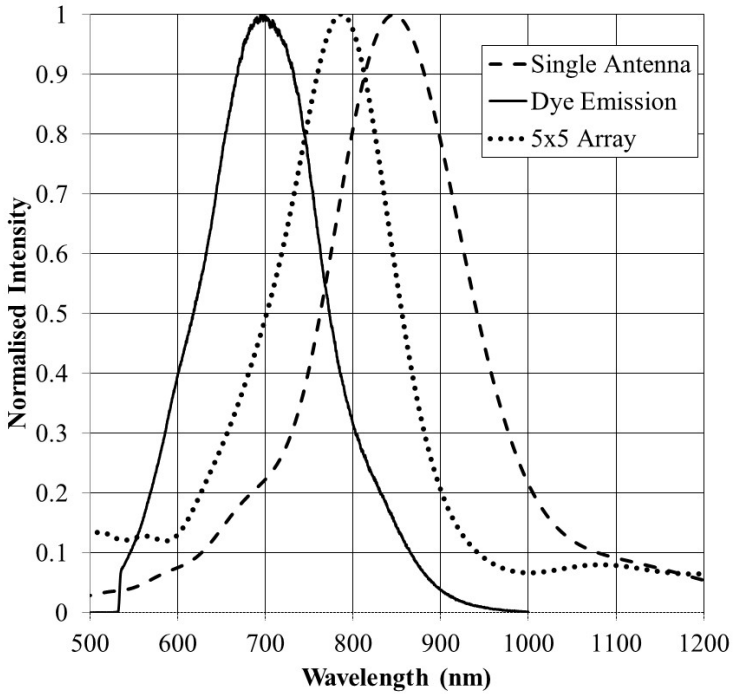

Figure 2 – Measured emission spectrum from LDS798 dye mixed with PMMA(solid line), and FDTD modelled resonances of a single (dashed line) and 5 x 5 array (dotted line) of dipole nanoantenna with dimensions matching those fabricated. The antennas are covered in a 250nm thick dielectric (n=1.485) to represent the dye/PMMA layer

To mix the dye and PMMA a solution is made consisting of acetone and toluene at a ratio of 2:1 to which 1.25% by mass of PMMA is added. Dye is then added at a concentration of 6.9×10^{-5}mol/L. The solution is then spin coated onto the surface of the sample at an acceleration of 5000 rev.s^{-2} to an angular velocity of 6000 revs.s^{-1} for 30 seconds. Assuming uniform coverage this concentration gives approximately 2-3 molecules present in the 50 nm gap, which for arms of 40 nm width and 50 nm thickness has a volume of 1×10^{-22} m^3

The fluorescence measurements were taken using a scanning confocal microscope in combination with a Renishaw Invia spectrometer equipped with a Peltier cooled CCD camera, which has a spectral resolution of 1 nm using 300 lines/mm grating. A x100 microscope lens was used with a numerical aperture, NA = 0.9 and a working distance of 300 μm. The dye molecules were optically pumped with a CW 532 nm Diode Pumped Solid State laser, which was focused to a ~350 nm spot on the surface with a power of 0.05 mW. The emission spectra were collected via the same lens, and all light with wavelength below 550 nm was filtered out. Spatially resolved measurements were taken using a motorised XYZ stage with 0.1 μm step size resolution. To measure the far-field radiation pattern both horizontal and vertical scans were performed through the centre of the array and each measurement point was separated by 100-200 nm.

Figure 3 shows a line a scan through the origin across both the horizontal (*x*)-axis of the antennas and the vertical (*y*)-axis of the antennas. The spectrum at each point was recorded and intensity between 600 nm and 750 nm was integrated, these data were normalised and plotted vs location of the scan. This plot reveals a number of interesting features, primarily the high fluorescence intensity over the nanoantenna array location, approximately between 14-17μm shown in Figure 3. This increase in recorded far-field intensity can be attributed to a combination of both focusing and Purcell enhancement as discussed earlier. Secondly, the widths of *x* and *y* intensity profiles from array location are different. This agrees with

beamshaping predicted by conventional RF antenna array theory. Since the *x*-pitch is larger than the *y*-pitch of the array the emission is expected to have a narrower beamwidth in the *x*-direction, this will be discussed in detail in the following section.

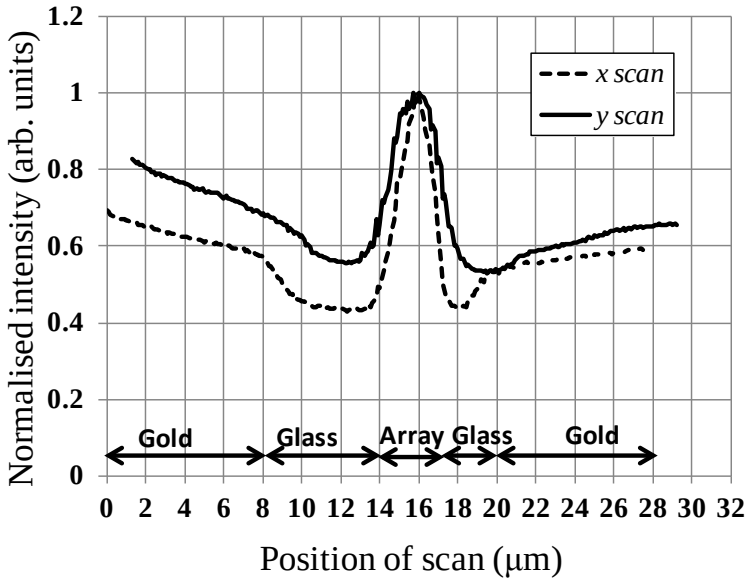

Figure 3 – Horizontal (x) and vertical (y) scans of fluorescence emission from the 5 x 5 array of dipole nanoantennas shown in figure 1 coated with LDS798 dye mixed with PMMA. Each scan consists of a number of spectra taken from a point every 0.1 μm with intensity integrated over a wavelength range of 600-750nm and then normalised.

3. Modelling

In order to understand the measured results the FDTD method (Lumerical FDTD solutions) was used to calculate radiation patterns and resonance wavelengths for two different arrays. Both 3 x 3 and 5 x 5 arrays are studied to show both comparisons with measured results and the impact of changing array size. Figure 4 shows the schematic layout of a 3 x 3 array. The simulation environment is 3-D and surrounded by perfectly matched layers (PMLs). The structures are coated with 250 nm of PMMA (n = 1.485) and on a glass substrate of n = 1.4, which extends into the negative z-direction PML, effectively making it infinite in that direction. The nanostructures are excited from above (positive z-direction) via a Total field/Scattered Field Gaussian plane wave, with wavelength centered at 700 nm. This type of source forms a box around the scattering structure and when the scattered field reaches the box the source energy is subtracted, leaving only the scattered field outside the box. A monitor is located above the source so only scattered radiation is detected. This monitor can be used to plot a number of important parameters, such as the reflection spectrum, field distribution and far-field radiation pattern. All far-field plots presented here were calculated at the peak resonance for that structure, where the peak resonance is calculated via the use of a probe located at 400 nm above the nanostructure.

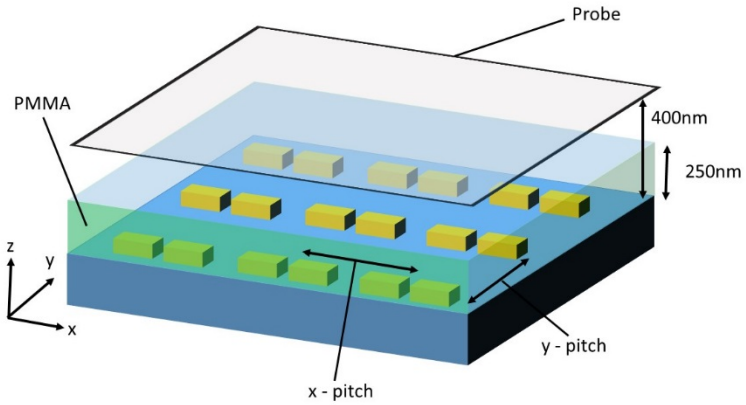

Figure 4 – A schematic of a PMMA coated 3x3 nanoantenna array.

For traditional RF antennas, the beamshape or radiation pattern has been studied for many decades and is well understood. Radiation patterns can be controlled by the shape of individual antennas, however, it is usual to produce arrays of antennas to give more control over the gain and directivity of the radiation pattern. One simple way one can utilise the extra control given by arrays is by varying the pitch between individual emitters along the long and short axis of the antennas. This variation in pitch effectively controls the interference between radiation from the individual elements and offers a large degree of control over the resulting beam shape [7].

In the field of plasmonics the idea of using arrays is beginning to gain momentum [9], [15]. In this section, the effects of pitch and array size are explored. If one considers making an array of plasmonic nanostructures then it should be possible to apply RF antenna array theory to the system. This is because, although each two-arm element in the array acts plasmonically, with the element spacing used here they are only electromagnetically coupled to adjacent two arm elements. An effective way to demonstrate control of the radiation pattern is to make an asymmetric beam in the farfield as fabricated and measured in section 2. As briefly mentioned earlier, it can be seen from Figure 3 that the beamshape of an array with an asymmetric pitch results in an asymmetric beamshape as expected from traditional RF theory. Figure 5 shows the FDTD simulation results for (a) a 5 x 5 array and (b) a 3 x 3 array with dimensions and pitches that match the array fabricated in section 2. It can be seen that good qualitative agreement is obtained between the measured and modelled results for the asymmetry of the beamwidths in the vertical and horizontal directions. It should be noted that it is not straightforward to convert the linear profile of Figure 3 into the angular space of the FDTD calculated far field. The measurement in Figure 3 is constructed from a series of point measurements where a pump laser spot illuminates the array and emitted fluorescence is collected through the same optics. The collection angle of NA = 0.9 lens is 108 degrees, so it must collect significant proportion of emitted radiation. However, the whole array is not emitting and the emitting area is defined by the size of the pump spot and any mutual coupling occurring between the array elements. Based on our spot size we estimate that when pumping the centre of the 5 x 5 array we have emission from a 3 x 3 array and an intensity profile is formed as beam spot moves across the larger array as shown in Figure 3. However, when pumping at the edge of the whole array a 1 x 3 array is emitting. In general, the 3 x 3 results show the significant increase in beamwidth that occurs as array size reduces, with smaller asymmetry ratio, compared with 5 x 5 case. While it is not possible to directly compare the experimental data with results of the simulations, they do illustrate a general trend in changing the beam shape due to asymmetry of the array pitches.

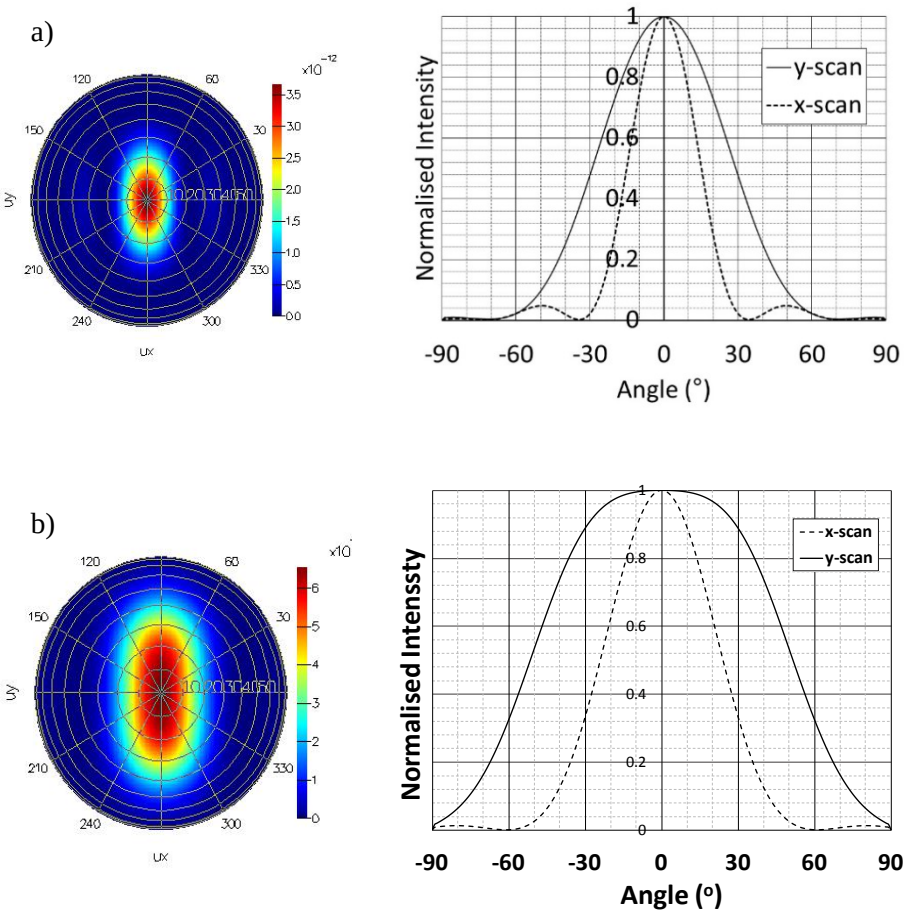

Figure 5 – The farfield radiation patterns and accompanying cross-sections of intensity from a) 5 x 5 array and b) 3 x 3 array both with the same dimensions as fabricated in section 2 and coated in a 250 nm PMMA layer of n=1.485.

		3x3 Array	5x5 Array
Beam Width	**x-scan**	50°	30°
	y-scan	102°	60°

Table 1 – A table summarising the FDTD calculated beam width at 50% peak for a 3x3 and 5x5 arrays in the absence of a PMMA layer. All arrays have an x and y-pitch of 450 and 230nm respectively

3.1 The Friis Formula and Intensity Enhancement

In this section we will use the well known Friis formula, shown in equation 1, to separate Purcell enhancement from antenna array focusing effects.

$$\frac{P_r}{P_t} = G_r G_t \left(\frac{\lambda}{4\pi d}\right)^2 \quad (1)$$

Where P_r is the received power, P_t is the transmitted power, G_r is the receiver Gain, G_t is the transmitter gain, d is the distance between transmit and receive antennas and λ is the wavelength. As discussed briefly earlier we have two measured cases as can be seen in Figure 3. We have received power over the array, P_{ra} and over bare glass, P_{rg}. In both cases d, λ and G_r are fixed, thus we can take the ratio of the two received powers and obtain equation 2:

$$\frac{P_{ra}}{P_{rg}} = \frac{P_{ta}}{P_{tg}} \frac{G_{ta}}{G_{tg}} \tag{2}$$

Where G_{tg} is the gain of emission from flat glass, G_{ta} is the array gain, P_{ta} is the power emitted in the array case and P_{tg} is the power emitted in the flat glass case. From equation 2 with knowledge of the gain with and without the array we can estimate the ratio of transmitted powers, which is in effect the Purcell enhancement for the array. It now remains to evaluate the gain with and without the array. With no array present the emission into air is expected to be very uniform, with no strongly directionality and thus we can assume the gain to be unity, i.e. omnidirectional emission. In the case of the array, we could attempt to estimate the gain directly from measured result shown in Figure 3, however the nature of this measurement is quite complex. For this reason we will use the calculated data from Figure 5(b) to estimate the gain for the 3 x 3 emitting array, as this approximates the excitation spot in the centre of the array, used in the fluorescence measurements.. From Figure 5(b) we have an x and y beamwidth and this can be used to estimate an array directivity, D from the following formula [16]:

$$D \approx \frac{32000}{\theta_x \theta_y} \tag{3}$$

where, θ_x and θ_y are half power beamwidths in degrees. This gives D of 6.27 for a 3 x 3 array using data in table 1. Here we are assuming an antenna efficiency of unity such that we can equate directivity D with gain G. While the FDTD calculation do include metal losses, accurately calculating gain is quite challenging and will be addressed in future work.

From Figure 3 we can calculate the ratio of P_{ra}/P_{rg} . If we compare the peak emission at the centre of array (scan position 16μm) to the averaged normalised intensity from the glass regions on either side of the peak, we obtain a ratio of approximately 2. Then using the array gain calculated above, G_{ta}= 6.27, we obtain an estimate for expected enhancement in emitted power in the presence of the array of 2/6.27 ≈ 0.32. This value is expected to be greater than 1 and we believe this is due to variety of the factors: i) efficiency losses related to the array fabrication challenges, ii) there may also be resonance detuning effects with respect to dye emission peak related to excited array size, iii) the small number of molecules in the antenna gaps could result in either no molecules being present or none being preferentially aligned resulting in much lower intensity enhancements. A number of other arrays with similar dimensions to that measured in Figure 3 were also investigated. Figure 6 shows the highest enhancement result we obtained. We calculated an average level normalised intensity on the glass to be 0.18 and this gives a highest observed enhancement factor of approximately 6, which results in an increase in emitted power due the array of 0.96.

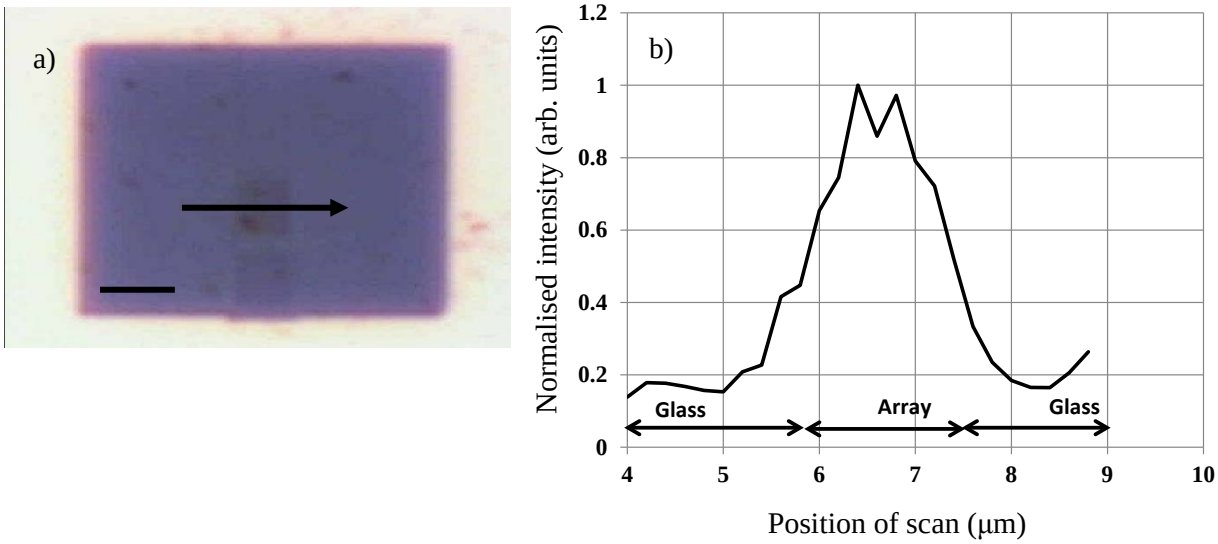

Figure 6 – (a) An image of the nanoantenna area with the scan path superimposed. Scale bar is 2μm (b) Confocal scan along the short axis of the array and intensity is integrated over the range of 600-750 nm.

These enhancement factors are much lower than others quoted in the literature, this is because we have not accounted for the fact that emission in the array case is coming from a very small mode volume, i.e., the very small gaps between the dipole antenna arms and the few molecules contained within these gaps. Thus to make a comparison between the bare glass and array cases we will calculate the emitting mode volume for each case and multiple our simple enhancement factor by this ratio.

It is a reasonable to assume that the intensity enhancement is primarily derived from molecules coupled to the array and therefore those that lie within the small mode volume of the antennas that make up the array. The mode volume of a single antenna is calculated via Lumerical FDTD solutions using equation 4 [17]:

$$V_m = \int \frac{\varepsilon E^2}{\max(\varepsilon E^2)} dV, \tag{4}$$

where V_m is the mode volume of a single antenna, E is electric field amplitude and ε is the permittivity of the medium.

The mode volume, which is different from the gap volume discussed earlier, was calculated for a single antenna element with a gap of 50 nm and an arm length, width and height of 100 nm, 40 nm and 50 nm respectively. The PMMA layer of n = 1.485 was included in the simulation along with the substrate. Assuming that the emission mainly comes from a 3 x 3 array within the pump spot, we obtain 2.49 x 10^{-23} m^3 for a single antenna and 22.4 x 10^{-23} m^3 for the 3 x 3 array. We will now modify the enhancement calculated from the Friis formula (1) by the ratio of the emission volumes for the array, V_a and non-array, V_g, respectively.

To calculate V_g it is necessary to know the lateral spot size of the lens along with its depth of field. The axial resolution of the confocal microscope was approximately 350 nm. As the vertical resolution is greater than the PMMA thickness which is estimated to be 250 nm, the total volume excited is approximated as a cylinder through the PMMA with a height of 250

nm and a diameter of 350 nm giving V_s = 2.40 x 10^{-20} m^3. This gives a ratio V_g/V_a= 107, resulting in a modified intensity enhancement for the case in Figure 6 of 107 x 0.96 = 102 times.

Conclusions

Thus the approach outlined here gives a reasonably straightforward approach of taking measured fluorescence emission data and with a knowledge of the array gain estimates the measured Purcell Enhancement, this is then further modified to include the very small emission volume of the array to give a useful figure-of-merit for use in fluorescence applications. It should be noted that while antenna efficiency is not included in the gain estimate, it is obviously included in the measured data and so can be seen as a very realistic estimate of Purcell enhancement in array structures.

This paper is one of the first demonstrations of use of planar arrays of nanostructures to obtain Purcell enhanced fluorescence emission whilst simultaneously focusing the radiation emitted to attain a Purcell enhancement of 0.96 and a mode volume corrected enhancement of 102 times. It is believed that this could be further increased if the resonant wavelength of the array was ideally aligned to the dye resonance. In real biosensing applications, the use of micro and nanofluidic channels and surface functionalization could be used to ideally align dye molecules in the high intensity gap regions, further increasing measured enhancements.

References

[1] A. Kinkhabwala, Z. Yu, S. Fan, Y. Avlasevich, K. Müllen, and W. E. Moerner, “Large single-molecule fluorescence enhancements produced by a bowtie nanoantenna,” Nat. Photonics, vol. 3, no. 11, pp. 654–657, Oct. 2009.

[2] A. Rose, T. B. Hoang, F. McGuire, J. J. Mock, C. Ciracì, D. R. Smith, and M. H. Mikkelsen, “Control of Radiative Processes Using Tunable Plasmonic Nanopatch Antennas,” Nano Lett., vol. 14, no. 8, pp. 4797–4802, Jul. 2014.

[3] E. M. Purcell, “Spontaneous Emission Probabilities at Radio Frequencies,” Proc. Am. Phys. Soc., vol. 69, no. 11 and 12, p. 681, 1946.

[4] A. G. Curto, G. Volpe, T. H. Taminiau, M. P. Kreuzer, R. Quidant, and N. F. van Hulst, “Unidirectional Emission of a Quantum Dot Coupled to a Nanoantenna,” Science, vol. 329, no. 5994, pp. 930–933, 2010.

[5] J. L. Stokes, Y. Yu, Z. H. Yuan, J. R. Pugh, M. Lopez-Garcia, N. Ahmad, and M. J. Cryan, “Analysis and design of a cross dipole nanoantenna for fluorescence-sensing applications,” J. Opt. Soc. Am. B, vol. 31, no. 2, pp. 302–310, Feb. 2014.

[6] H. Kollmann, X. Piao, M. Esmann, S. F. Becker, D. Hou, C. Huynh, L.-O. Kautschor, G. Bösker, H. Vieker, A. Beyer, A. Gölzhäuser, N. Park, R. Vogelgesang, M. Silies, and C. Lienau, “Toward Plasmonics with Nanometer Precision: Nonlinear Optics of Helium-Ion Milled Gold Nanoantennas,” Nano Lett., vol. 14, no. 8, pp. 4778–4784, Jul. 2014.

[7] D. M. Pozar, Microwave Engineering, 3rd Editio. Wiley & Sons, 2005.

[8] G. M. Akselrod, C. Argyropoulos, T. B. Hoang, C. Ciracì, C. Fang, J. Huang, D. R. Smith, and M. H. Mikkelsen, “Probing the mechanisms of large Purcell enhancement in plasmonic nanoantennas,” Nat. Phot., vol. 8, no. 11, pp. 835–840, Nov. 2014.

[9] D. Dregely, K. Lindfors, M. Lippitz, N. Engheta, M. Totzeck, and H. Giessen, “Imaging and steering an optical wireless nanoantenna link,” Nat Commun, vol. 5, Jul. 2014.
[10] “Platypus Technologies.” [Online]. Available: http://www.platypustech.com/.
[11] J. L. Stokes, “Beamshaping and Fluorescent Enhancement via Plasmonic Nanostructures and Arrays,” PhD Thesis, University of Bristol, 2014.
[12] D. Lu, J. J. Kan, E. E. Fullerton, and Z. Liu, “Enhancing spontaneous emission rates of molecules using nanopatterned multilayer hyperbolic metamaterials,” Nat Nano, vol. 9, no. 1, pp. 48–53, Jan. 2014.
[13] “Photonic Solutions.” [Online]. Available: http://www.photonicsolutions.co.uk/.
[14] “MicroChem PMMA data sheet.” [Online]. Available: http://microchem.com/pdf/PMMA_Data_Sheet.pdf.
[15] T. Niu, W. Withayachumnankul, B. S.-Y. Ung, H. Menekse, M. Bhaskaran, S. Sriram, and C. Fumeaux, “Experimental demonstration of reflectarray antennas at terahertz frequencies,” Opt. Express, vol. 21, no. 3, pp. 2875–2889, Feb. 2013.
[16] Constantine A. Balanis, *Antenna Theory: Analysis and Design*, John Wiley & Sons 2012
[17] K. Srinivasan, M. Borselli, O. Painter, A. Stintz, and S. Krishna, “Cavity Q, mode volume, and lasing threshold in small diameter AlGaAs microdisks with embedded quantum dots,” Opt. Express, vol. 14, no. 3, pp. 1094–1105, 2006.